

1 **Expanding the cultivable human archaeome: *Methanobrevibacter intestini***  
2 **sp. nov. and strain *Methanobrevibacter smithii* “GRAZ-2” from human feces**

3

4 Viktoria Weinberger<sup>1†</sup>, Rokhsareh Mohammadzadeh<sup>1†</sup>, Marcus Blohs<sup>1</sup>, Kerstin Kalt<sup>1</sup>,  
5 Alexander Mahnert<sup>1</sup>, Sarah Moser<sup>1</sup>, Marina Cecovini<sup>1</sup>, Polona Mertelj<sup>1</sup>, Tamara Zurabishvili<sup>1</sup>,  
6 Jacqueline Wolf<sup>3</sup>, Tejas Shinde<sup>1</sup>, Tobias Madl<sup>2,4</sup>, Hansjörg Habisch<sup>4</sup>, Dagmar Kolb<sup>5,6</sup>,  
7 Dominique Pernitsch<sup>5</sup>, Kerstin Hingerl<sup>5</sup>, William Metcalf<sup>7</sup>, Christine Moissl-Eichinger<sup>1,2\*</sup>

8

9 <sup>1</sup> D&R Institute of Hygiene, Microbiology and Environmental Medicine, Medical University of Graz,  
10 Graz, Austria

11 <sup>2</sup> BioTechMed Graz, Graz, Austria

12 <sup>3</sup> Research Group Metabolomics, Leibniz Institute DSMZ-German Collection of Microorganisms and  
13 Cell Cultures GmbH, Braunschweig, Germany.

14 <sup>4</sup> Otto Loewi Research Center, Medicinal Chemistry, Research Unit Integrative Structural Biology,  
15 Medical University of Graz, Graz, Austria

16 <sup>5</sup> Core Facility Ultrastructure Analysis, Medical University of Graz, Graz, Austria

17 <sup>6</sup> Gottfried Schatz Research Center, Cell Biology, Histology and Embryology, Medical University of  
18 Graz, Graz, Austria

19 <sup>7</sup> Department of Microbiology, University of Illinois, Urbana, Illinois, USA

20

21 \*Corresponding author

22 [christine.moissl-eichinger@medunigraz.at](mailto:christine.moissl-eichinger@medunigraz.at)

23

24 Repositories: The genome of GRAZ-2 is available through BioProject ID PRJNA1067514. The 16S rRNA  
25 gene sequence of WWM1085 is available through NCBI GenBank PP338268.

26

27 <sup>†</sup>These authors contributed equally: Viktoria Weinberger, Rokhsareh Mohammadzadeh

28

29 **Abstract**

30 Two mesophilic, hydrogenotrophic methanogens, WWM1085 and *M. smithii* GRAZ-2 were  
31 isolated from human fecal samples. WWM1085 was isolated from an individual in the USA,  
32 and represents a novel species with in the genus *Methanobrevibacter*. *M. smithii* GRAZ-2 (=  
33 DSM 116045) was retrieved from fecal samples of a European, healthy female and represents  
34 a novel strain within this genus. Both *Methanobrevibacter* representatives form non-  
35 flagellated, short rods with variable morphologies and the capacity to form filaments. Both  
36 isolates showed the typical fluorescence of F<sub>420</sub> and methane production.

37 Compared to *M. smithii* GRAZ-2, WWM1085 did not accumulate formate when grown on H<sub>2</sub>  
38 and CO<sub>2</sub>. The optimal growth conditions were at 37°C, and pH 7. Full genome sequencing  
39 revealed a genomic difference of WWM1085 to the type strain of *M. smithii* PS (type strain;  
40 DSM 861), with 93.55% ANI and major differences in the sequence of its *mcrA* gene (3.3%  
41 difference in nucleotide sequence). Differences in the 16S rRNA gene were very minor and  
42 thus distinction based on this sequence might not be possible. *M. smithii* GRAZ-2 was  
43 identified as a novel strain within the *Methanobrevibacter* genus (ANI 99.04 % to *M. smithii*  
44 PS).

45 Due to the major differences of WWM1085 and *M. smithii* type strain PS in phenotypic,  
46 genomic and metabolic features, we propose *M. intestini* sp. nov. as a novel species with  
47 WWM1085 as the type strain (DSM 116060T = CECT 30992).

48 **Keywords:** *Methanobrevibacter smithii*, *Methanobrevibacter intestini*, fecal methanogens,  
49 human archaeome

## 51 Introduction

52 *Methanobrevibacter* species are widespread and have been found in numerous host  
53 microbiomes. They exhibit remarkable adaptability in engaging with both animal hosts and  
54 non-archaeal elements within their microbiome. By metabolizing diverse small fermentation  
55 byproducts, these species effectively facilitate and support various syntrophic interactions.  
56 They stand out as the predominant archaea thriving in the gastrointestinal tracts of not only  
57 several animals (1–3).

58 Among these species, *M. smithii* (with four isolates currently available, source: Global catalog  
59 of microorganisms, Nov 2023, <https://gcm.wdcm.org/>), represents the most prevalent  
60 archaeon within the human gut, exhibiting an average relative abundance of up to 2% in  
61 individuals with high methane emission levels in their breath (4).

62 It's worth noting that the *M. smithii* type strain PS (DSM 861; hereby referred to as: "*M. smithii*  
63 PS"), was initially isolated from sewage samples rather than human feces (5). A contamination  
64 of the sewage sample with human feces cannot be excluded, in particular as the  
65 gastrointestinal tract is the most favorable habitat for *M. smithii*. In contrast, strain ALI (DSM  
66 2375; hereby referred to as: "*M. smithii* ALI") (6) is considered as one of the first publicly  
67 available *M. smithii* strains described and isolated directly from human fecal samples.

68 Additionally, a recent discovery indicated that *M. smithii* encompasses two distinct clades,  
69 tentatively labeled as *smithii* and *smithii\_A* within the GTDB taxonomy (Rinke et al., 2021).  
70 This differentiation was further corroborated through genomic analyses and the  
71 incorporation of numerous metagenome-assembled genomes (MAGs) from studies on the  
72 human microbiome, confirming the taxonomic separation between *smithii* and *smithii\_A* (8).

73 It was found that the median genome size of *smithii\_A* slightly surpasses that of *smithii* (1.9  
74 Mbp compared to 1.7 Mbp), while showing an average nucleotide identity (ANI) of 93.95%.  
75 Despite this variance, key genes linked to methanogenesis were shared between both strains.  
76 The *mcrA* gene exhibited an average amino acid sequence difference of 2.15% (8), a potential  
77 marker for distinguishing these clades using molecular methods (9). Following these  
78 observations, *smithii\_A* was tentatively designated as a distinct species namely, *Candidatus*  
79 *Methanobrevibacter intestini*.

80 *Cand. M. intestini* is represented by WWM1085 (formerly recognized as a strain of *M. smithii*),  
81 which was initially isolated from human stool in the presence of CO<sub>2</sub>-H<sub>2</sub> as a carbon and  
82 energy source (Chibani et al., 2022; Jennings et al., 2017). This species demonstrates extensive  
83 distribution and a notably high prevalence among the human population, accounting for  
84 approximately 90.01% ((11)). In the present paper, we further describe *Methanobrevibacter*  
85 *intestini* as a novel species within the *Methanobrevibacter* genus using comparative 16S rRNA  
86 and genome sequencing, culture-based methods, electron microscopy, lipidomics, and  
87 metabolomics. We provide this *Methanobrevibacter intestini* strain (WWM1085) as a new  
88 addition to the culture collection (DSM 116060) of anaerobic archaea found in humans.  
89 Moreover, we characterize another newly isolated strain of *M. smithii* called *M. smithii* GRAZ-  
90 2.

91

92 **Materials and methods**

93 **Sources of microorganisms.**

94 Strain WWM1085 (= DSM 116060 = CECT 30992) was enriched by the Department of  
95 Microbiology, University of Illinois, Urbana, Illinois, United States, from a fecal sample (Mayo  
96 Clinic Minnesota, biome number 101159) in the presence of CO<sub>2</sub> and H<sub>2</sub> as a carbon and  
97 energy source. Further details are provided in the draft genome sequence announcement by  
98 Jennings et al. (Jennings et al., 2017). The enrichment was subcultured and purified via  
99 antibiotic treatment to a pure culture in 2021 at the Medical University of Graz, Austria. In  
100 detail, the growth medium (MpT1, see below) was supplemented with streptomycin sulfate  
101 (10 mg/ml) and penicillin G potassium salt (10 mg/ml) at a volume ratio of 1:100 (0.2 ml of  
102 the antibiotics mixture in a volume of 20 ml of medium).

103 *M. smithii* GRAZ-2 was isolated from a stool sample of a healthy female aged 42 at Medical  
104 University of Graz, Graz, Austria in 2018 in presence of CO<sub>2</sub> and H<sub>2</sub> as a carbon and energy  
105 source. This strain is also currently available in DSMZ (= DSM 116045) (German Collection of  
106 Microorganisms and Cell Cultures GmbH, Braunschweig, Germany).

107 *M. smithii* ALI (= DSM 2375) was obtained from the DSMZ and was used for comparative  
108 analysis.

109 **Ethical approval**

110 Sampling of the human fecal sample was evaluated and approved by the local ethics  
111 committee (27-151 ex 14/15). Before participation, the participant signed an informed  
112 consent.

113

114 **Enrichment and isolation of strain GRAZ-2.**

115 The stool sample was collected from a fresh fecal sample with an ESwab (COPAN Diagnostics  
116 Inc., Italy). The collection fluid, which keeps anaerobic microorganisms alive, was transferred  
117 to ATCC medium 1340 (MS medium for methanogens, see below), supplemented with  
118 ampicillin (100 µg/mL), streptomycin (100 µg/mL), tetracycline (10 µg/mL) and nystatin (20  
119 µg/mL). Methane production in the culture's headspace was verified after visible growth  
120 (turbidity and microscopy) using a methane sensor (BCP-CH4 sensor, BlueSens).

121 Enrichment of methanogens was achieved via fluorescence-activated cell sorting (FACS)  
122 exploiting the auto-fluorescence of the cofactor F<sub>420</sub>. FACS was performed at the ZMF Core  
123 Facility Molecular Biology in Graz, Austria. For detection of the F<sub>420</sub> fluorescence, the violet  
124 laser (405 nm) and the bandpass filter 450/40 of the FACSaria III system (Becton Dickinson)  
125 were used. During the short sorting process, cells were kept and sorted into reduced medium.  
126 500,000 events were collected and re-grown in liquid MS medium (see below).

127 Subsequently, the culture was plated on solid MS medium (1.5 % agar, w/v) in Hungate tubes  
128 using the roll-tube method as described (12). A single colony was picked and re-grown in liquid  
129 media. To further ensure purity, serial dilutions were performed.

130 **Growth media.**

131 Standard archaeal medium (13) was used to grow all isolates, with some modifications. This  
132 medium contained the following constituents (l<sup>-1</sup> distilled water): 0.45 g NaCl, 5 g NaHCO<sub>3</sub>, 0.1  
133 g MgSO<sub>4</sub>.7H<sub>2</sub>O, 0.225 g KH<sub>2</sub>PO<sub>4</sub>, 0.3 g K<sub>2</sub>HPO<sub>4</sub>.3H<sub>2</sub>O, 0.225 g (NH<sub>4</sub>)<sub>2</sub>SO<sub>4</sub>, 0.060 g CaCl<sub>2</sub>.2H<sub>2</sub>O, 2

134 ml (NH<sub>4</sub>)<sub>2</sub>Ni(SO<sub>4</sub>)<sub>2</sub> solution (0.1% w/v), 2 ml FeSO<sub>4</sub>.7 H<sub>2</sub>O solution (0.1% w/v in 0.1 M H<sub>2</sub>SO<sub>4</sub>),  
135 and 0.7 ml resazurin solution (0.1% w/v). These compositions were then supplemented with  
136 1 ml of each 10x Wolfe's vitamin and 10x mineral solutions (13). Media was then  
137 deoxygenated with N<sub>2</sub> and 0.75 g L-cysteine was added under anaerobic conditions. pH was  
138 adjusted to 7.0 if necessary. 20 ml of liquid was then aliquoted into 100 ml serum bottles,  
139 sealed with rubber stopper and aluminum cap, and pressurized with H<sub>2</sub>/CO<sub>2</sub> (4:1) before  
140 autoclaving. Before use, 0.001 g/ml of yeast extract and 0.001 g/ml sodium acetate were  
141 added to the media.

142 For growth of WWM1085, MpT1 medium, based on AM-5 (14), was used with some  
143 modifications. Modified MpT1 medium had the following compositions (l<sup>-1</sup> distilled water): 1  
144 g NaCl, 0.5 g KCl, 0.19 g MgCl<sub>2</sub>, 0.1 g CaCl<sub>2</sub> x 2 H<sub>2</sub>O, 0.3 g NH<sub>4</sub>Cl, 0.2 g KH<sub>2</sub>PO<sub>4</sub>, 0.15 g Na<sub>2</sub>SO<sub>4</sub>, 2  
145 g casamino acids, 2 g yeast extract, 0.082 g sodium acetate. Then, 1 ml trace element solution  
146 (1.2 ml HCl (12.5 M), 0.01 g MnCl<sub>2</sub> x 4 H<sub>2</sub>O, 0.019 g CoCl<sub>2</sub> x 6 H<sub>2</sub>O, 0.0144 g ZnSO<sub>4</sub> x 7 H<sub>2</sub>O,  
147 0.0002 g CuCl<sub>2</sub> x 2H<sub>2</sub>O, 0.003 g H<sub>3</sub>BO<sub>3</sub>, 0.0024 g NiCl<sub>2</sub> x 6 H<sub>2</sub>O, 0.0036 g Na<sub>2</sub>MoO<sub>4</sub> x 2 H<sub>2</sub>O in  
148 150 ml distilled water), 20 µl of selenite-tungstate solution (2 g NaOH, 0.01 g Na<sub>2</sub>SeO<sub>3</sub>.5H<sub>2</sub>O,  
149 and 0.017 g Na<sub>2</sub>WO<sub>4</sub>.2H<sub>2</sub>O dissolved in 50 ml distilled water) and 0.7 ml resazurin solution  
150 (0.1% w/v) were added. Media was deoxygenated with N<sub>2</sub> and subsequently, 0.24 g L-Cysteine  
151 and 2.52 g NaHCO<sub>3</sub> were added. 20 ml of medium was distributed in 100-ml serum bottle and  
152 was then sealed and pressurized with H<sub>2</sub>/CO<sub>2</sub> (4:1). After autoclaving, 0.2 ml of the following  
153 were added to each bottle under anoxic conditions: methanol (50 mM), dithiothreitol (0.154  
154 g/L), Na-formate (0.034 g/L) / Na-coenzyme M (0.01 g/L) and vitamin solution (3 mg Biotin, 3  
155 mg Folic acid, 15 mg Vitamin B6, 7.5 mg Vitamin B1, 7.5 mg Vitamin B2, 7.5 mg Nicotinic acid,  
156 7.5 mg DL-Panthothenic acid, 1.5 mg Vitamin B12, 7.5 mg P-Aminobenzoic acid, 0.3 g Choline

157 chloride dissolved in 150 ml distilled water) were added to each bottle under anaerobic  
158 conditions. The pH was adjusted to 7.0 if applicable.

159 All growth experiments were carried out in triplicates under static conditions at 37 °C unless  
160 mentioned otherwise.

161 **Scanning electron microscopy (SEM)**

162 For scanning electron microscopy, cells were mounted on coverslips, fixed with 2 % (w/v)  
163 paraformaldehyde in 0.1 M phosphate buffered saline, pH 7.4 and 2.5% glutaraldehyde in 0.1  
164 M phosphate buffered saline, pH 7.4, and dehydrated stepwise in a graded ethanol series.  
165 Samples were post-fixed with 1 % osmium tetroxide for 1 h at room temperature and  
166 subsequently dehydrated in graded ethanol series (30-96 % and 100 % (v/v) EtOH). Further,  
167 Hexamethyldisilane (HMDS (Merck | Sigma - Aldrich) was applied. Coverslips were placed on  
168 stubs covered with a conductive double coated carbon tape. The images were taken with a  
169 Sigma 500VP FE-SEM with a SEM Detector (Zeiss Oberkochen) operated at an acceleration  
170 voltage of 5 kV.

171 **Optimum pH and temperature**

172 The 100-ml serum bottles, each containing 20 ml of modified standard archaeal medium (for  
173 all tested isolates) and MpT1 (only for WWM1085), were inoculated with 2.5% (v/v) fresh  
174 cultures. Growth, measured in terms of OD at 600 nm, and methane production were  
175 monitored daily for 10 days to assess the impact of pH and temperature on growth. Methane  
176 levels were quantified using a gas sensor (BluSens, Germany), and data integration and  
177 analysis were performed using the provided BacVis Gas Formation software.

178 To explore the effect of pH on growth, media with different pH values ranging from 5 to 8  
179 with 0.5 intervals, as well as pH values of 9, 10, and 11, were prepared by adjusting with  
180 varying amounts of 0.1 M NaOH or 0.1 M HCl. The pH values of the media were checked daily  
181 for potential alterations (pH indicator strips, VWR, Germany) and were maintained constant.  
182 The optimum pH was determined at 37°C.

183 For the determination of the optimum temperature, cultures were incubated at various  
184 temperatures (20, 30, 35, 37, 39, 40, and 50 °C), while pH was kept constant at 7. Temperature  
185 was monitored continuously using a temperature logger (Sensor Blue, Brifit) inside the  
186 incubator. Both pH and temperature experiments for WWM1085 were conducted in modified  
187 standard archaeal medium and MpT1.

188

#### 189 **Culture purity check and sequencing**

190 Cultures were routinely checked for purity using microscopy, PCR and Sanger sequencing.  
191 Microscopic examination of the cells was performed using a Nikon microscope equipped with  
192 a fluorescence attachment and a UV excitation filter. Extracted DNA was subjected to PCR  
193 targeting the archaea *mcrA* (forward primer sequence: 5' CAACCCAGACATTGGTACTCCT 3',  
194 reverse: 5' GCTGGGGTGATGACAGTTCT 3') and the bacterial 16S rRNA gene (primers 341F  
195 and 1391R) (15,16). Media blanks and no-template controls served as negative controls.

#### 196 **Nanopore sequencing**

197 The studied archaeal species underwent Nanopore sequencing using the MinION Mk1C  
198 system (Oxford Nanopore Technologies plc., UK) according to the protocols as detailed in  
199 (nanoporetech.com). To summarize, DNA extraction was done according to the  
200 manufacturer's protocol (Invitrogen™ PureLink™ Microbiome DNA Purification Kit, Thermo

201 Fisher Scientific Inc, USA), and subsequently, Nanodrop 2000c spectrophotometer (Thermo  
202 Fisher Scientific Inc., USA) and an Invitrogen™ Qubit™ 3 Fluorometer (Thermo Fisher  
203 Scientific Inc., USA) were used to confirm the quality and concentration of the extracted DNA.  
204 In addition, gel electrophoresis was employed for checking DNA fragmentation. DNA was then  
205 stored at -20 °C for further analyses.

206 In the process of preparing the library, DNA underwent repair utilizing the NEBNext  
207 Companion Module (New England Biolabs GmbH, GER). Subsequently, it was prepared for  
208 sequencing on a chemistry version 14 flow cell (R10.4.1, FLO-MIN114) following the Ligation  
209 sequencing gDNA – Native Barcoding Kit 24 V14 (SQK-NBD114.24) as outlined by the  
210 guidelines of the manufacturer as detailed in (nanoporetech.com).

211 **DNA-based comparisons**

212 16S rRNA genes were retrieved from isolates' genomes using the ContEst16S tool created by  
213 EzBioCloud (17) (Supplementary Table S1). The genomes were retrieved from own  
214 sequencing (GRAZ-2) or public databases (NQLD00000000 for WWM1085, all other accession  
215 numbers are provided in Supplementary Table S1).

216 Some genomes contained multiple copies of the 16S rRNA genes; in such a case, all were  
217 included in the subsequent analyses. Alignment of the sequences was performed via Muscle  
218 ((18,19), implemented in Mega11 (standard settings of MEGA11; (20)). All aligned 16S rRNA  
219 genes were manually trimmed to the same length. Pairwise distance estimation was  
220 performed using the standard settings. The matrix is available in Supplementary Table 2. The  
221 16S rRNA gene-based tree was created via SILVA SINA using the FastTree option (model: GTR,  
222 rate model for likelihoods: Gamma; variability profile: Archaea; Positional variability filter,  
223 domain Archaea) (21–23).

224 *mcrA* genes were retrieved through MAGE genoscope ((24); Supplementary Table 3), a  
225 platform for genomic comparison. Genes were aligned through Muscle (see above) and  
226 pairwise distance estimation was calculated using the standard settings of Mega11. The  
227 matrix is provided in Supplementary Table 4.

228 The probability of whether one or two isolated *Methanobrevibacter* strains represent novel  
229 species was tested using JSpeciesWS (25). The Average Nucleotide Identity (ANI) was  
230 calculated against all isolates listed in Supplementary Table 5-6, and those provided by the  
231 curated reference database GenomesDB. This tool also provided the GC content of each  
232 genome.

233 The whole genome tree was calculated using MAGE genoscope (24) and the integrated  
234 “Clustering Genomes” function. The tree is constructed from the Mash distance matrix  
235 (26,27) and computed dynamically using a rapid neighbour joining algorithm. For details,  
236 please refer to the tutorial of MAGE genoscope.

### 237 **Lipid and carbohydrate profile analyses by mass spectrometry**

238 Intact polar lipids were extracted from freeze-dried material (approx. 30 mg) using a modified  
239 Bligh and Dyer extraction as described previously (28–31). Briefly, two extractions each were  
240 performed using methanol/dichloromethane (DCM)/50 mM phosphate buffer pH 7-8 (2:1:0.8  
241 v/v/v) and methanol/DCM/0.3 M trichloroacetic acid pH 2-3 (2:1:0.8 v/v/v). Combined  
242 supernatants were adjusted to a ratio of methanol/DCM/50 mM phosphate buffer of (2:1:0.9  
243 v/v/v) by adding DCM and phosphate buffer, before the DCM phase was collected. The  
244 remaining mixture was additionally extracted twice with DCM and the combined DCM phases

245 were evaporated to dryness. For HPLC-MS/MS analysis dried extracts were recovered in  
246 hexane/isopropanol/water (718:271:10 v/v/v).

247 Archaeal lipids were separated on a YMC-Triart Diol column (150 x 2.0 mm, 1.9  $\mu$ m particles)  
248 and analyzed in positive ESI mode by mass spectrometry on an Agilent 6545 Q-ToF mass  
249 spectrometer (Agilent, Waldbronn, Germany) as described previously (28,32). Mass spectra  
250 were recorded in the mass range of m/z 300-2000. Core lipids were identified by the exact  
251 masses of their [M+H]<sup>+</sup> ions.

252 For analysis of lipid associated sugars, lipid extracts were prepared as described above and  
253 hydrolyzed according to (33) with slight modifications. Briefly, dried extracts were resolved in  
254 1 ml 2 N H<sub>2</sub>SO<sub>4</sub> and incubated for 2 h at 100 °C. Afterwards the samples were chilled on ice  
255 and neutralized by adding 2 N NaOH (final pH 6-8). After centrifugation the supernatant was  
256 evaporated to dryness.

257 For GC-MS analysis of sugar residues tried extracts were reconstituted in 1 ml methanol and  
258 filtered through a Nylon spin filter to remove excess salt. The remaining supernatant was  
259 mixed with 10  $\mu$ l of a 4 % ribitol-methanol solution and dried under a stream of nitrogen. In  
260 addition, non-hydrolyzed extracts were analyzed to detect any residual free sugars in the lipid  
261 extracts. Derivatization and GC-MS analysis was performed as described previously (34). Data  
262 analysis was performed with the MetaboliteDetector software (35) as described previously  
263 (36).

264 **Quantification of metabolic activity by NMR spectroscopy**

265 Five replicates for each of the studied archaeal cultures (in MS medium and yeast extract  
266 supplement (see above)) at different time points (72h, 168h, and 240h), were subjected to

267 analysis utilizing Nuclear Magnetic Resonance (NMR) spectroscopy, following the  
268 methodology outlined before (4). Briefly, a methanol-water mixture (2:1) was employed to  
269 eliminate proteins from samples followed by centrifugation. Subsequently, the supernatant  
270 was lyophilized, re-dissolved in sodium phosphate-buffered NMR buffer also containing 4.6  
271 mM 3-trimethylsilyl propionic acid-2,2,3,3,-d4 sodium salt (TMSP) as internal standard, and  
272 subsequently transferred to NMR tubes. NMR analysis was then conducted on a Bruker  
273 Avance Neo NMR spectrometer running at 600 MHz and equipped with a TXI probe head at  
274 310 K and Topsin 4.3 software (Bruker GmbH, Rheinstetten, Germany). The obtained spectra  
275 (cmpgpr1d/Carr-Purcell-Meiboom-Gill pulse sequence with 128 scans) were further  
276 processed using MATLAB 2014b (Mathworks, Natick, MA, USA), aligned, and normalized by  
277 probabilistic quotient normalization (37,38). For absolute quantification of carbonic acids,  
278 known peaks of substances of aligned raw spectra were integrated using trapezium  
279 subtraction for baseline correction (39), and eventually normalized on their respective proton  
280 number, J-coupling pattern, and TMSP integral of the sample in order to calculate their molar  
281 concentrations.

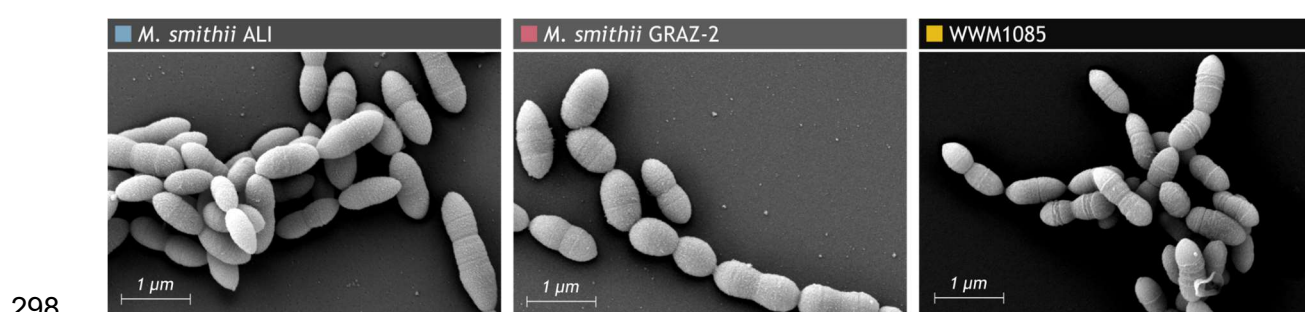
282

283 **Results and discussion**

284 Based on our findings, the investigated archaeal strains, namely WWM1085 and *M. smithii*  
285 GRAZ-2, along with *M. smithii* DSM 2375, which was used for comparison, exhibit unique  
286 features discerned through our culture-based, genomics, and metabolomics methods. These  
287 distinctive characteristics are outlined in Supplementary Table 1 and elaborated upon in the  
288 subsequent sections.

289 **Morphology**

290 WWM1085 cells appeared morphologically similar to both *M. smithii* ALI and *M. smithii* GRAZ-  
291 2 albeit being slightly shorter. In general, they measure 0.16-0.43  $\mu\text{m}$  in width and 0.29-0.54  
292  $\mu\text{m}$  in length and appear mostly in the form of short rods with rounded ends (Fig. 1). Similar  
293 to *M. smithii* ALI and *M. smithii* GRAZ-2, not only they occurred in single cells, but were also  
294 observed more frequently in pairs, short chains or long filaments. Pili or flagella were not  
295 detected, but some cells appeared fluffy on their surface. All isolates showed F<sub>420</sub>  
296 fluorescence, which is typical for methanogenic archaea, when observed under fluorescence  
297 microscopy (excitation 420 nm). No cells were observed in media controls.



299 **Fig 1.** Scanning electron micrograph of *Methanobrevibacter smithii* ALI, *Methanobrevibacter smithii* GRAZ-2,  
300 and WWM1085.  
301

302 **Substrates and nutritional requirements**

303 WWM1085 underwent growth testing in two media, namely MS and MpT1 media, with  
304 various substrates to assess potential variations in its nutritional requirements compared to  
305 *M. smithii* ALI and *M. smithii* GRAZ-2. At pH 7 and 37°C, this strain demonstrated optimal  
306 growth in both media and reached high cell density after 72 hours (2.5% (v/v) inoculation),  
307 utilizing H<sub>2</sub>/CO<sub>2</sub> as its energy source. No growth was observed when growth media were  
308 exposed to oxygen.

309 **Optimum pH range for growth and methane production**

310 WWM1085 (in both media), along with *M. smithii* ALI, and *M. smithii* GRAZ-2 constantly  
311 produced methane across a broad pH spectrum (6.5 - 10) (Table. 1). On the basis of methane  
312 production and OD600, the optimum pH was found to be 7-7.5 in the MS medium. In modified  
313 MpT1, WWM1085 showed the optimal growth at a pH range of 6.5-7. The type strain *M.*  
314 *smithii* PS showed an optimal pH range between pH 6.9 and 7.4 (40). None of the isolates,  
315 showed growth at pH 5 and 11.

316

317

318

319

320

321 **Table 1.** Optimal pH and temperature for the growth of the studied strains. Growth was determined  
322 by measuring OD600 in the growth medium and the ability of the strains to produce methane. (+) minimal growth; (++) moderate growth; (+++) optimal growth; (-) no growth; ND: Not determined.

324

Strain		<i>M. smithii</i> ALI	<i>M. smithii</i> GRAZ-2	WWM1085	
Growth condition	Medium	MS	MS	MS	Modified MpT1
	Temperature (°C)	20	⊕	⊕	⊕
pH	30	⊕	⊕	⊕⊕	⊕⊕
	35	⊕	⊕	⊕⊕⊕	⊕⊕
	37	⊕⊕	⊕⊕	⊕⊕⊕	⊕⊕⊕
	39	⊕⊕⊕	⊕⊕⊕	⊕⊕⊕	⊕⊕⊕
	40	⊕⊕⊕	⊕⊕⊕	⊕	⊕⊕
	50	⊕	⊕	⊕	⊕
	5	⊕	⊕	⊕	⊕
6.5	⊕	⊕	⊕⊕	⊕⊕⊕	
7	⊕⊕⊕	⊕⊕⊕	⊕⊕⊕	⊕⊕	
8	⊕⊕⊕	⊕⊕⊕	⊕⊕⊕	⊕⊕	
9	⊕⊕	⊕⊕	⊕⊕	⊕	
10	⊕⊕	⊕	⊕	⊕	ND
11	⊕	⊕	⊕	⊕	

325

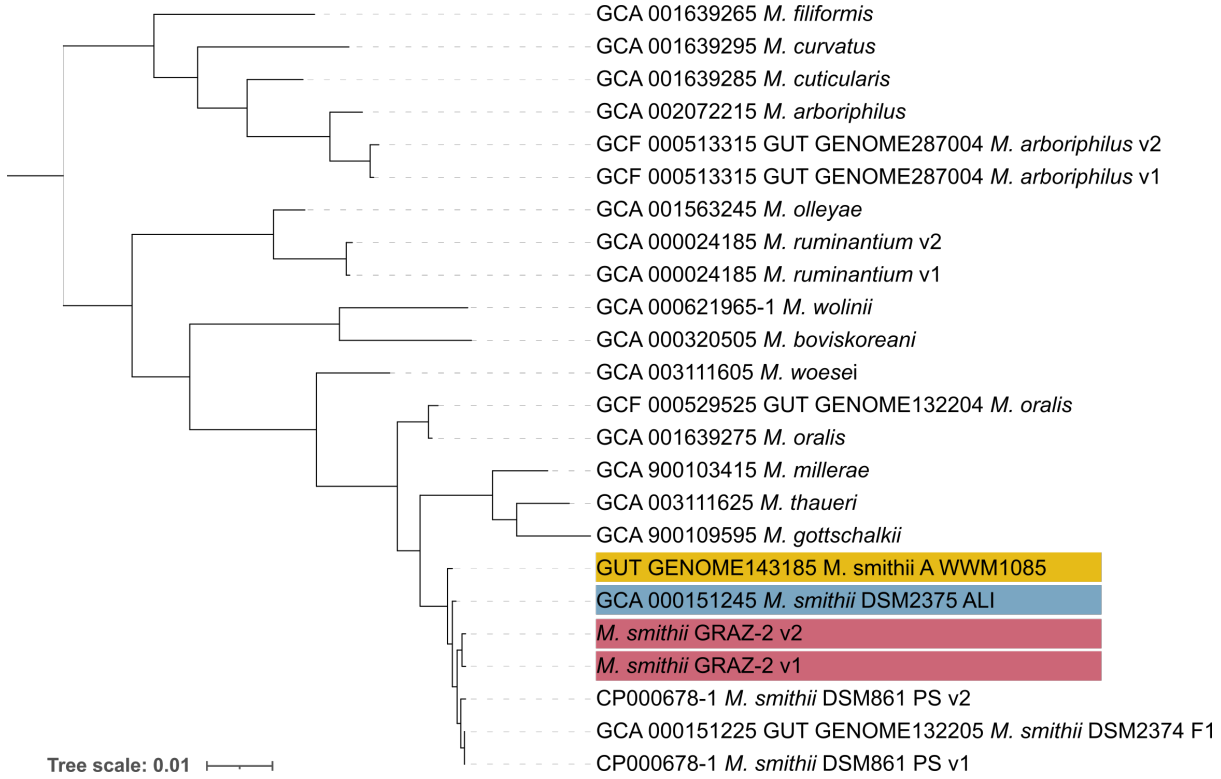
326 **Optimum temperature range for growth and methane production**

327 All three isolates exhibited growth and methane production within a temperature range of  
328 30-40°C (30, 35, 37, 39, and 40°C) (Table 1). In the modified standard archaeal medium, the  
329 optimum temperature range for *M. smithii* ALI, *M. smithii* GRAZ-2, and WWM1085 was  
330 determined to be 39-40°C, 39-40°C, and 35-39°C, respectively (Table 1). Notably, WWM1085  
331 demonstrated the identical optimal growth at 35-39°C in the modified MpT1 medium, too. In

332 summary, WWM1085 displayed a broader but lower temperature range for moderate or  
333 optimal growth as compared to the other two strains. No growth was observed under more  
334 extreme temperature conditions (20°C or 50°C) for any of the isolates. The type strain *M.*  
335 *smithii* PS showed an optimal temperature range between 37 and 39°C (40).

336 **Phylogenetic relationships**

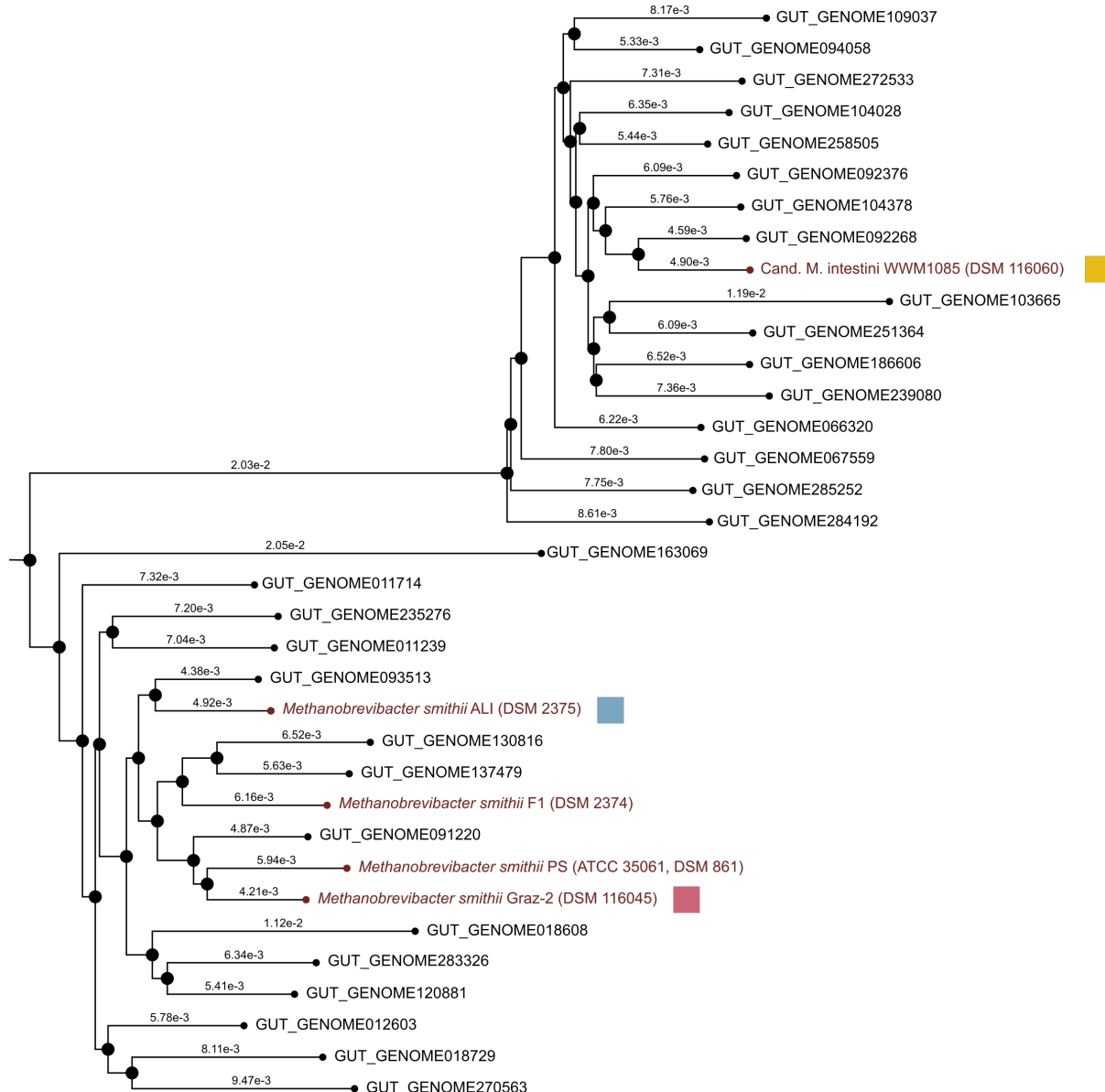
337 The full-length 16S rRNA gene analysis of WWM1085 showed small variations as compared  
338 to closely related *Methanobrevibacter smithii* isolates (*M. smithii* ALI: 0.135%, *M. smithii* PS:  
339 0.203%; Supplementary Table S2). These slight discrepancies pose a challenge for  
340 differentiating the isolates solely through 16S rRNA gene sequencing. It's important to  
341 highlight that these sequence variations arose within a homopolymeric sequence region  
342 (multiple T), and at this juncture, we cannot dismiss the possibility of differences arising from  
343 sequencing artifacts or technical issues. The 16S rRNA gene of *M. smithii* GRAZ-2 was found  
344 to be highly similar to the genes of *M. smithii* PS and *M. smithii* ALI (difference: 0.068%;  
345 Supplementary Table S2) (Fig. 2).



361 DSMZ collection (30.3% as opposed to 31.0-31.3%). When performing pairwise ANI  
362 calculations, the similarity values of WWM1085 against strains from GenomesDB and the  
363 culture collection consistently fell well below the species threshold (cutoff: 95%). The closest  
364 relatives were found to be *M. smithii* ALI (ANI: 93.04%) and *M. smithii* PS (ANI: 93.55%).

365 Consequently, it can be concluded that WWM1085 represents a distinct species within the  
366 *Methanobrevibacter* genus. However, it is important to note that despite these genomic  
367 differences, the disparities in the 16S rRNA gene are subtle, and in some cases, imperceptible  
368 in amplicon-based studies.

369 *M. smithii* GRAZ-2 showed the closest relationship to *M. smithii* PS (ANI: 99.04 %) and  
370 therefore does not represent a novel species within the *Methanobrevibacter* genus (all  
371 information given in Supplementary Table S6). For visualization, a genome-based tree is  
372 provided in Fig. 3.



373

374 **Fig. 3.** Neighbour Joining tree, calculated for genomes of *Methanobrevibacter* isolates (which are  
375 available in culture collections and are shown in dark red), and respective MAGs (Chibani et al., 2022)  
376 from the *M. smithii* clade. Representative genomes of the recently identified clade centered around  
377 WWM1085 (highlighted with a yellow square) are designated as “Mbb\_smithii\_A” based on the current  
378 GTDB classification. Consistent and stable clustering of the two *Methanobrevibacter* clades was  
379 observed. Pink square indicates *M. smithii* GRAZ-2, blue square *M. smithii* ALI. Distances based on the  
380 Mash distance matrix (24) are correlated to the average nucleotide identity (ANI) such as  $D \approx 1 - ANI$ .

381 WWM1085 shares its closest genetic relationship with the readily accessible *M. smithii* strain,  
382 known as *M. smithii* ALI. Notably, this particular strain was isolated from human  
383 gastrointestinal samples as well (in contrast to the available *M. smithii* PS, which was isolated

384 from sewage). Consequently, throughout this study, WWM1085 and *M. smithii* GRAZ-2 were  
385 specifically compared to *M. smithii* ALI.

386 **Polar lipid composition and lipid-associated sugars**

387 Major detected lipids were largely congruent across species and strains, with archaeol  
388 ( $C_{43}H_{88}O_3$ ) being the most prevalent lipid (Relative abundance for *M. smithii* ALI: 83.93%;  
389 WWM1085: 72.57%; and *M. smithii* GRAZ-2: 93.85%), followed by Caldarchaeol ( $C_{86}H_{172}O_6$ )  
390 (*M. smithii* ALI: 13.65%; WWM1085: 26.37%; *M. smithii* GRAZ-2: 5.81%), and cyclic archaeol  
391 ( $C_{43}H_{86}O_3$ ) (*M. smithii* ALI: 0.65%; WWM1085: 1.06%; *M. smithii* GRAZ-2: 0.34%). Traces of  
392 glycerol dialkyl glycerol tetraether lipids (GDGT-1) or H-shaped caldarchaeol were found in *M.*  
393 *smithii* ALI (1.77%), but not in the other strains.

394 Lipid-associated sugar profiles were very similar for all strains with glucose being most  
395 prevalent, accompanied by minor amounts of fructose, rhamnose, ribose and xylose.

396 **Comparative genomics and metabolomics**

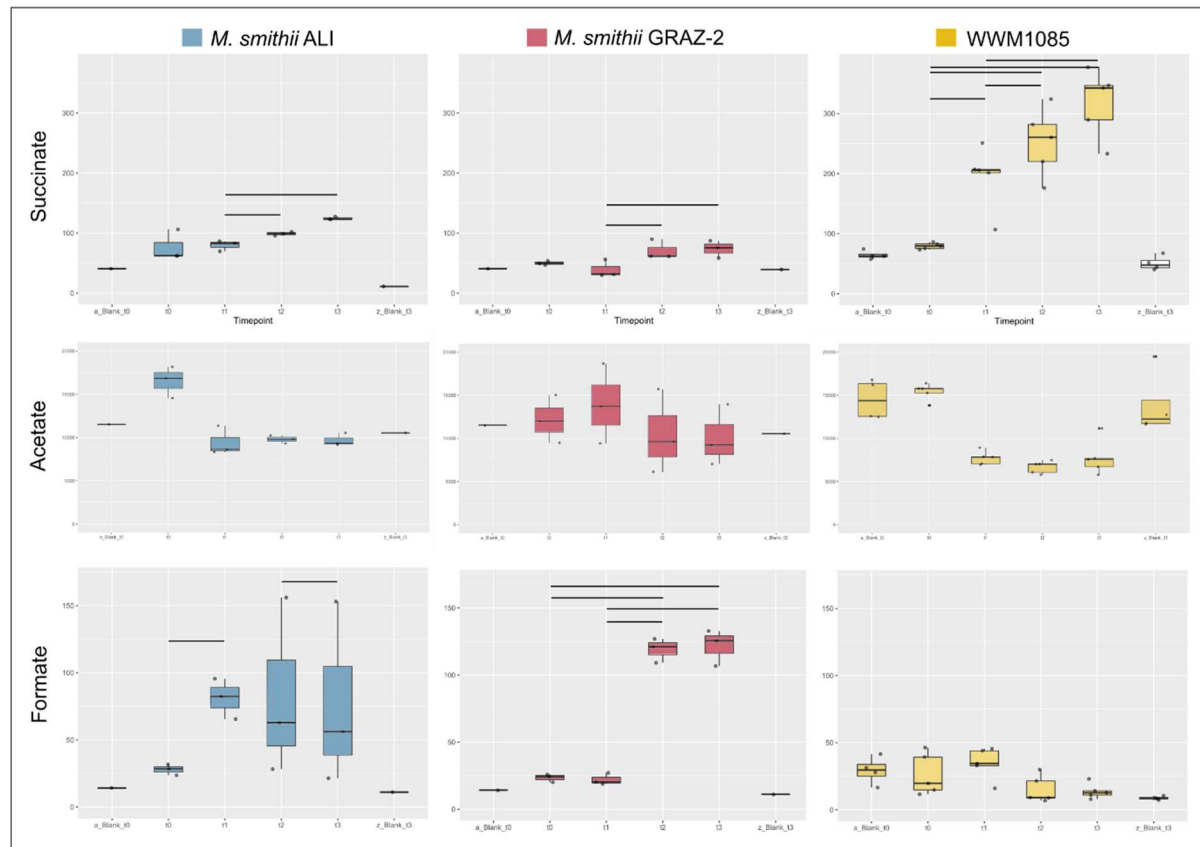
397 Detailed genomic comparisons of WWM1085 with available *M. smithii* genomes are provided  
398 in our earlier publication (8), indicating several differences. For instance, WWM1085 does not  
399 possess modA/B for molybdate transport. The *M. smithii*\_A genomes (including those from  
400 MAGs) were further characterized by additional unique membrane/cell-wall-associated  
401 proteins, such as adhesin-like proteins, surface proteins and a number of uncharacterized  
402 membrane proteins/transporters (8). Notably, *M. smithii* GRAZ-2 and the WWM1085 genome  
403 contained the ABC.FEV.P/S/A iron transport system (EC 3.6.3.34), which was distinctive to all  
404 other tested genomes, indicating a potential adaptation towards the human gut environment,  
405 where iron is a highly-demanded resource.

406 Utilizing NMR-based metabolomics, the turnover of metabolites was examined among three  
407 strains (*M. smithii* ALI, *M. smithii* GRAZ-2, and WWM1085) in a medium containing yeast  
408 extract. All strains reached the stationary phase after 72 h (*M. smithii* ALI and WWM1085) or  
409 at the latest, after 168 h (*M. smithii* GRAZ-2) of growth (growth curves shown in  
410 Supplementary Fig. 1).

411 All strains exhibited a notable and expected statistically significant uptake of acetate and  
412 production of succinate, which was highest in the WWM1085 culture (4-fold increase; Fig. 4)  
413 (Supplementary Table S7).

414 Unlike the *M. smithii* cultures, WWM1085 did not exhibit formate accumulation in the  
415 medium. Specifically, there was a notable and substantial increase in formate accumulation  
416 for *M. smithii* GRAZ-2, reaching a fivefold increase (Fig. 4).

Compound	DSM 2375 ALI	GRAZ-2	WWM1085
Succinate ( $\text{C}_4\text{H}_6\text{O}_4$ )	⊕	⊕	⊕⊕⊕⊕
Acetate ( $\text{C}_2\text{H}_3\text{O}_2$ )	⊖	⊖	⊖
Formate ( $\text{CH}_2\text{O}_2$ )	⊕⊕	⊕⊕⊕⊕⊕	⊖



418 **Fig. 4.** Metabolic dynamics and variability in various compounds among the studied  
419 *Methanobrevibacter* strains in MS medium supplemented with yeast extract. Concentrations in  $\mu\text{M/L}$ .  
420 Upper panel (table): The symbols indicate statistically significant changes over time, with the number  
421 of symbols reflecting the fold change (e.g., 5 symbols denote a 5-fold change or more). The gray  
422 symbol signifies a statistical trend ( $p=0.05X$ ). The symbol "-" denotes no change. Lower panel: Boxplots  
423 of the respective measurements (all original data provided in Supplementary Table S7). It's  
424 noteworthy that media blanks did not exhibit any statistically significant changes in compound levels.

425

426 All biological properties of the tested strains, including *M. smithii* PS are provided in Table 2.

427

428

429 **Table 2.** Distinguishing features among the strains *M. smithii* ALI, *M. smithii* GRAZ-2, and WWM1085.

430 \* Description for type strain *M. smithii* PS taken from (40) and (42). ND: Not determined, med: medium.

431

432

Trait	<i>M. smithii</i> PS (type strain) *	<i>M. smithii</i> ALI	<i>M. smithii</i> GRAZ-2	WWM1085 (MS med.)	WWM1085 (MpT1 med.)
DSM indication number	DSM 861	DSM 2375	DSM 116045	DSM 116060	
Cell shape	Short, lancet-shaped to oval cocci	Coccobacillus, short rods	Coccobacillus, short rods	Coccobacillus, short rods	
Cell size, width, length	0.5-1.0 µm 1.0-1.5 µm	0.22-0.54 µm 0.26-0.77 µm	0.18-0.58 µm 0.33-1.46 µm	0.16-0.43 µm 0.29-0.54 µm	
Genome size	1.85 Mbp	1.71 Mbp	1.79 Mbp	1.9 Mbp	
DNA G+C content (mol%)	31.03	31.28	31.11	30.30	
N50	1.85 Mbp	226.2 kb	1.79 Mbp	240.4 kb	
Number of contigs	1	24	1	16	
Number of CDS	1838	1712	1906	1875	
Number of tRNAs	34	33	34	34	
Lipid profile	mostly (cald-)archaeol	mostly archaeol	mostly archaeol	mostly archaeol	
Temperature range (°C)	ND	30-40	30-40	30-40	
Optimal temperature (°C)	37-39	39-40	39-40	35-39	37-40
pH range	ND	6.5-10	6.5-10	6.5-10	6.5-9
Optimal pH	6.9-7.4	7-7.5	7-7.5	7-7.5	6.5-7
growth on formate as sole H <sub>2</sub> source	Possibly	No	No	No	
CO <sub>2</sub> /H <sub>2</sub> as carbon and energy source	Yes	Yes	Yes	Yes	
Isolation source	Sludge	Human	Human	Human	

433

434

435 **Description of *Methanobrevibacter intestini* sp. nov.**

436

437 *Methanobrevibacter intestini* (in.tes.ti'ni. L. gen. n. *intestini*, of the gut). Coccobacillus with  
438 slightly tapered or rounded ends, about 0.16-0.43  $\mu\text{m}$  in width and 0.29-0.54  $\mu\text{m}$  in length,  
439 occurring mostly in pairs or short chains. The DNA GC content is 30.30 mol%. Optimum  
440 temperature: 35-40°C; optimum pH 6.5-7.5. Strictly anaerobic. Grows and produces methane  
441 from  $\text{H}_2$  and  $\text{CO}_2$ . Requires acetate and additional organics (e.g. yeast extract) for growth. Can  
442 not grow on formate as a sole electron source. Genome comparisons with type species *M.*  
443 *smithii* PS revealed numerous differences including an average nucleotide identity of 93.55%.  
444 With such, WWM1085 represents a novel species within the *Methanobrevibacter* genus, and  
445 is the first isolated representative. Strain WWM1085 was isolated from human feces from an  
446 US American individual. The type strain WWM1085<sup>T</sup> (=DSM 116060, CECT 30992). The  
447 GenBank accession number of its genome is NQLD00000000.

448

449 **Sequencing data**

450 The GenBank accession number of the genome of WWM1085 is NQLD00000000. The genome  
451 of GRAZ-2 is available through BioProject ID PRJNA1067514. The 16S rRNA gene sequence of  
452 WWM1085 is available through NCBI GenBank PP338268.

453

454 **Funding information**

455 This research was funded in whole or in part by the Austrian Science Fund (FWF) [grants P  
456 32697, P 30796, COE 7, 10.55776/P28854, 10.55776/I3792, 10.55776/DOC130, and  
457 10.55776/W1226]; Austrian Research Promotion Agency (FFG) grants 864690 and 870454;  
458 the Integrative Metabolism Research Center Graz; the Austrian Infrastructure Program  
459 2016/2017; the Styrian Government (ZukunftsFonds, doc.fund program); the City of Graz; and

460 BioTechMed-Graz (flagship project). For open access purposes, the author has applied a CC  
461 BY public copyright license to any author-accepted manuscript version arising from this  
462 submission.

463

464 **Conflicts of interest**

465 The authors declare that there is no conflict of interest regarding the publication of this  
466 research paper.

467

468 **Acknowledgements**

469 We would like to acknowledge the computational resources of the MedBioNode at the  
470 Medical University of Graz, as funded by the Austrian Federal Ministry of Education, Science  
471 and Research, Hochschulraum-Strukturmittel 2016 grant as part of BioTechMed Graz, and the  
472 support of the ZMF team at the Core Facility Computational Bioanalytics (Medical University  
473 of Graz). We further thank Birgit Grün and Gesa Martens (DSMZ) for excellent technical  
474 assistance.

475

476

477

478 **References**

- 479 1. Borrel G, Brugère JF, Gribaldo S, Schmitz RA, Moissl-Eichinger C. The host-  
480 associated archaeome. Vol. 18, *Nature Reviews Microbiology*. Nature Research;  
481 2020. p. 622–36.
- 482 2. Youngblut ND, Reischer GH, Dauser S, Maisch S, Walzer C, Stalder G, et al.  
483 Vertebrate host phylogeny influences gut archaeal diversity. *Nat Microbiol* [Internet].  
484 2021 Nov 26;6(11):1443–54. Available from: <https://www.nature.com/articles/s41564-021-00980-2>
- 485 3. Thomas CM, Desmond-Le Quéméner E, Gribaldo S, Borrel G. Factors shaping the  
486 abundance and diversity of the gut archaeome across the animal kingdom. *Nat  
487 Commun.* 2022 Jun 10;13(1):3358.
- 488 4. Kumpitsch C, Fischmeister FPS, Mahnert A, Lackner S, Wilding M, Sturm C, et al.  
489 Reduced B12 uptake and increased gastrointestinal formate are associated with  
490 archaeome-mediated breath methane emission in humans. *Microbiome*. 2021;9(1):1–  
491 18.
- 492 5. Bryant MP, Tzeng SF, Robinson IM, Joiner AEJ. Nutrient requirements of  
493 methanogenic bacteria. In: Pohland FG, editor. *Anaerobic biological treatment  
494 processes*. Amer. Chem. Soc.; 1971. p. 23–40.
- 495 6. Miller TL, Wolin MJ. Fermentation by the human large intestine microbial community  
496 in an in vitro semicontinuous culture system. *Appl Environ Microbiol* [Internet]. 1981  
497 [cited 2024 Jan 26];42(3):400–7. Available from:  
498 <https://journals.asm.org/doi/10.1128/aem.42.3.400-407.1981>
- 499 7. Rinke C, Chuvochina M, Mussig AJ, Chaumeil PA, Davín AA, Waite DW, et al. A  
500 standardized archaeal taxonomy for the Genome Taxonomy Database. *Nat Microbiol*.  
501 2021;1–14.
- 502 8. Chibani CM, Mahnert A, Borrel G, Almeida A, Werner A, Brugère JF, et al. A  
503 catalogue of 1,167 genomes from the human gut archaeome. *Nat Microbiol*. 2022 Jan  
504 30;7(1):48–61.
- 505 9. Luton PE, Wayne JM, Sharp RJ, Riley PW. The mcrA gene as an alternative to 16S  
506 rRNA in the phylogenetic analysis of methanogen populations in landfill b bThe  
507 GenBank accession numbers for the mcrA sequences reported in this paper are  
508 AF414034–AF414051 (see Fig. 2) and AF414007–AF414033 (environmental isolates  
509 in Fig. 3). *Microbiology (N Y)*. 2002 Nov 1;148(11):3521–30.
- 510 10. Jennings ME, Chia N, Boardman LA, Metcalf WW. Draft genome sequence of  
511 *Methanobrevibacter smithii* Isolate WWM1085, obtained from a human stool sample.  
512 *Genome Announc*. 2017;5(39):e01055-17.
- 513 11. Mohammadzadeh R, Mahnert A, Duller S, Moissl-Eichinger C. Archaeal key-residents  
514 within the human microbiome: characteristics, interactions and involvement in health  
515 and disease. *Curr Opin Microbiol*. 2022 Jun 1;67:102146.
- 516 12. Hungate RE. Chapter IV A Roll Tube Method for Cultivation of Strict Anaerobes.  
517 *Methods in Microbiology*. 1969 Jan 1;3(PART B):117–32.
- 518 13. Balch WE, Fox GE, Magrum LJ, Woese CR, Wolfe RS. Methanogens: reevaluation of  
519 a unique biological group. *Microbiol Rev*. 1979;43(2):260.
- 520 14. Paul K, Nonoh JO, Mikulski L, Brune A. “*Methanoplasmatales*,” *Thermoplasmatales*-  
521 related archaea in termite guts and other environments, are the seventh order of  
522 methanogens. *Appl Environ Microbiol*. 2012;78(23):8245–53.

524 15. Walker JJ, Pace NR. Phylogenetic Composition of Rocky Mountain Endolithic  
525 Microbial Ecosystems. *Appl Environ Microbiol* [Internet]. 2007 Jun [cited 2024 Jan  
526 26];73(11):3497. Available from: [/pmc/articles/PMC1932665/](https://PMC1932665/)

527 16. Klindworth A, Pruesse E, Schweer T, Peplies J, Quast C, Horn M, et al. Evaluation of  
528 general 16S ribosomal RNA gene PCR primers for classical and next-generation  
529 sequencing-based diversity studies. *Nucleic Acids Res*. 2013 Jan;41(1):e1–e1.

530 17. ContEST16S tool. <https://www.ezbiocloud.net/tools/contest16s>. 2024. ContEst16S  
531 tool .

532 18. Edgar RC. MUSCLE: multiple sequence alignment with high accuracy and high  
533 throughput. *Nucleic Acids Res*. 2004 Mar 8;32(5):1792–7.

534 19. Edgar RC. MUSCLE: a multiple sequence alignment method with reduced time and  
535 space complexity. *BMC Bioinformatics*. 2004 Aug 19;5(1):113.

536 20. Tamura K, Stecher G, Kumar S. MEGA11: Molecular Evolutionary Genetics Analysis  
537 Version 11. *Mol Biol Evol* [Internet]. 2021 Jun 25 [cited 2024 Feb 13];38(7):3022–7.  
538 Available from: <https://dx.doi.org/10.1093/molbev/msab120>

539 21. Pruesse E, Peplies J, Glöckner FO. SINA: accurate high-throughput multiple  
540 sequence alignment of ribosomal RNA genes. *Bioinformatics*. 2012;28(14):1823–9.

541 22. Price MN, Dehal PS, Arkin AP. FastTree: Computing Large Minimum Evolution Trees  
542 with Profiles instead of a Distance Matrix. *Mol Biol Evol*. 2009 Jul 1;26(7):1641–50.

543 23. Quast C, Pruesse E, Yilmaz P, Gerken J, Schweer T, Yarza P, et al. The SILVA  
544 ribosomal RNA gene database project: improved data processing and web-based  
545 tools. *Nucleic Acids Res*. 2013 Jan;41(D1):D590–6.

546 24. Vallenet D, Calteau A, Dubois M, Amours P, Bazin A, Beuvin M, et al. MicroScope: an  
547 integrated platform for the annotation and exploration of microbial gene functions  
548 through genomic, pangenomic and metabolic comparative analysis. *Nucleic Acids  
549 Res* [Internet]. 2020 Jan 8 [cited 2024 Feb 13];48(D1):D579–89. Available from:  
550 <https://dx.doi.org/10.1093/nar/gkz926>

551 25. Richter M, Rosselló-Móra R, Oliver Glöckner F, Peplies J. JSpeciesWS: a web server  
552 for prokaryotic species circumscription based on pairwise genome comparison.  
553 *Bioinformatics* [Internet]. 2016 Mar 15 [cited 2024 Feb 13];32(6):929–31. Available  
554 from: <https://dx.doi.org/10.1093/bioinformatics/btv681>

555 26. Ondov BD, Treangen TJ, Melsted P, Mallonee AB, Bergman NH, Koren S, et al.  
556 Mash: fast genome and metagenome distance estimation using MinHash. *Genome  
557 Biol*. 2016;17(1):1–14.

558 27. Konstantinidis KT, Tiedje JM. Genomic insights that advance the species definition for  
559 prokaryotes. *Proceedings of the National Academy of Sciences*. 2005 Feb  
560 15;102(7):2567–72.

561 28. Hofmann M, Norris PR, Malik L, Schippers A, Schmidt G, Wolf J, et al. Metallosphaera  
562 javensis sp. nov., a novel species of thermoacidophilic archaea, isolated from a  
563 volcanic area. *Int J Syst Evol Microbiol*. 2022 Oct 17;72(10).

564 29. Weber Y, Sinninghe Damsté JS, Hopmans EC, Lehmann MF, Niemann H. Incomplete  
565 recovery of intact polar glycerol dialkyl glycerol tetraethers from lacustrine suspended  
566 biomass. *Limnol Oceanogr Methods*. 2017 Sep;15(9):782–93.

567 30. Lengger SK, Hopmans EC, Sinninghe Damsté JS, Schouten S. Impact of sedimentary  
568 degradation and deep water column production on GDGT abundance and distribution  
569 in surface sediments in the Arabian Sea: Implications for the TEX86  
570 paleothermometer. *Geochim Cosmochim Acta*. 2014 Oct;142:386–99.

571 31. Bligh EG, Dyer WJ. A RAPID METHOD OF TOTAL LIPID EXTRACTION AND  
572 PURIFICATION. *Can J Biochem Physiol*. 1959 Aug 1;37(8):911–7.

573 32. Besseling MA, Hopmans EC, Boschman RC, Sinnighe Damsté JS, Villanueva L.  
574 Benthic archaea as potential sources of tetraether membrane lipids in sediments  
575 across an oxygen minimum zone. *Biogeosciences*. 2018 Jul 4;15(13):4047–64.

576 33. Schumann P. Peptidoglycan Structure. In 2011. p. 101–29.

577 34. Will SE, Henke P, Boedeker C, Huang S, Brinkmann H, Rohde M, et al. Day and  
578 Night: Metabolic Profiles and Evolutionary Relationships of Six Axenic Non-Marine  
579 Cyanobacteria. *Genome Biol Evol*. 2019 Jan 1;11(1):270–94.

580 35. Hiller K, Hangebrauk J, Jäger C, Spura J, Schreiber K, Schomburg D.  
581 MetaboliteDetector: Comprehensive Analysis Tool for Targeted and Nontargeted  
582 GC/MS Based Metabolome Analysis. *Anal Chem*. 2009 May 1;81(9):3429–39.

583 36. Neumann-Schaal M, Hofmann JD, Will SE, Schomburg D. Time-resolved amino acid  
584 uptake of *Clostridium difficile* 630Δerm and concomitant fermentation product and  
585 toxin formation. *BMC Microbiol*. 2015 Dec 18;15(1):281.

586 37. Dieterle F, Ross A, Schlotterbeck G, Senn H. Probabilistic quotient normalization as  
587 robust method to account for dilution of complex biological mixtures. Application in <sup>1</sup>H  
588 NMR metabonomics. *Anal Chem*. 2006 Jul;78(13):4281–90.

589 38. Bohus E, Coen M, Keun HC, Ebbels TMD, Beckonert O, Lindon JC, et al. Temporal  
590 Metabonomic Modeling of L-Arginine-Induced Exocrine Pancreatitis. *J Proteome Res*.  
591 2008 Oct 3;7(10):4435–45.

592 39. Hedjazi L, Gauguier D, Zalloua PA, Nicholson JK, Dumas ME, Cazier JB.  
593 mQTL.NMR: An Integrated Suite for Genetic Mapping of Quantitative Variations of <sup>1</sup>H  
594 NMR-Based Metabolic Profiles. *Anal Chem*. 2015 Apr 21;87(8):4377–84.

595 40. Balch, WE, Fox GE, Magrum LJ, Woese CR, Wolfe RS. Methanogens: reevaluation  
596 of a unique biological group. *Microbiol Rev [Internet]*. 1979 Jun [cited 2024 Feb  
597 13];43(2):260–96. Available from: <https://journals.asm.org/journal/mr>

598 41. Almeida A, Nayfach S, Boland M, Strozzi F, Beracochea M, Shi ZJ, et al. A unified  
599 catalog of 204,938 reference genomes from the human gut microbiome. *Nat  
600 Biotechnol*. 2021;39(1):105–14.

601 42. Sprott GD, Brisson JR, Dicaire CJ, Pelletier AK, Deschatelets LA, Krishnan L, et al. A  
602 structural comparison of the total polar lipids from the human archaea  
603 *Methanobrevibacter smithii* and *Methanospaera stadtmanae* and its relevance to the  
604 adjuvant activities of their liposomes<sup>11</sup>Publication number 42395 of the National  
605 Research Council of Canada. *Biochimica et Biophysica Acta (BBA) - Molecular and  
606 Cell Biology of Lipids*. 1999 Sep;1440(2–3):275–88.

607